

Broadband-dielectric-spectroscopy study of molecular dynamics in a mixture of itraconazole and glycerol in glassy, smectic-A, and isotropic phases

M. Rams-Baron ^{1,2,*} D. Kramarczyk ^{1,2} J. Knapik-Kowalczyk^{1,2} B. Hachula,³ A. Kocot,⁴ and M. Paluch^{1,2}

¹*August Chelkowski Institute of Physics, University of Silesia, 75 Pulku Piechoty 1, 41-500 Chorzow, Poland*

²*Silesian Center for Education and Interdisciplinary Research, 75 Pulku Piechoty 1a, 41-500 Chorzow, Poland*

³*Institute of Chemistry, University of Silesia, Szkolna 9, 40-006 Katowice, Poland*

⁴*Institute of Materials Engineering, University of Silesia, 75 Pulku Piechoty 1a, 41-500 Chorzow, Poland*



(Received 14 February 2021; accepted 17 August 2021; published 9 September 2021)

Itraconazole (ITZ) is a thermotropic liquid crystal that exhibits isotropic, nematic, and smectic phases on cooling towards the glass transition upon melting. Over the years, new aspects regarding the liquid-crystalline ordering of this antifungal drug were systematically revealed. It has been shown recently that the temperature range of individual mesophases in ITZ can be modified by adding a small amount of glycerol (GLY). Moreover, above the critical concentration of 5% w/w, a smectic to nematic transition can be avoided. Here we go one step further, and we used broadband dielectric spectroscopy to investigate the new phase behavior of the ITZ-GLY mixture (5% w/w). To confirm the phase transformations of the ITZ-GLY mixture, differential scanning calorimetry was also employed. The analysis of molecular dynamics of the ITZ-GLY mixture in the glassy and isotropic phases revealed features similar to those observed for neat ITZ. Two relaxation processes were identified in the smectic-A phase, with similar temperature dependence, most likely related to the fast rotations around the long axis of a molecule. Additionally, the derivative analysis revealed another low-frequency process hidden under DC conductivity ascribed to the slow rotations about a short axis. We will show that the differences in the molecular organization in the smectic-A and isotropic phases leave a clear fingerprint on the temperature behavior of relaxation times and other dielectric parameters, such as DC conductivity and dielectric strength, for which a pretransition effect has been detected.

DOI: [10.1103/PhysRevE.104.034702](https://doi.org/10.1103/PhysRevE.104.034702)

I. INTRODUCTION

The remarkable properties of liquid crystals (LCs) are a manifestation of their hybrid nature, combining the features of solids and liquids. A fusion of seemingly contradictory properties, i.e., fluid molecular mobility with long-range ordering typical for crystal, is responsible for the success and enormous interest that liquid-crystalline materials and their singular properties have aroused in the last century [1,2]. The most recognizable industrial application of LCs is the production of liquid-crystal displays in various electronic devices, but the actual scientific and technological potential of LCs goes well beyond that [3].

The internal order of a mesophase governs the physical properties of LCs. In the thermotropic LCs, the temperature (or equivalently pressure) is the primary thermodynamic variable controlling the emergence of particular liquid-crystalline phases with their inherent patterns of molecular arrangement [3]. The most common are nematic and smectic phases. In the former, the molecules tend to roughly arrange in the same direction (along with the director), while in the latter, they organize additionally into layers leading to a state with a higher order [2]. There are several ways to adjust the sequence of mesophases to achieve new properties desired in

specific applications [4–7]. One of them is to design binary systems of LCs with nonmesogenic excipients, in which the temperature of phase transitions and, thus, the properties of the system are different from those observed for individual components. For example, the small addition of methanol to a 4-cyano-4'-pentylbiphenyl (5CB) allows one to systematically lower the temperature of isotropic to nematic transition (T_{I-N}) from 308 to 274 K [8]. T_{I-N} may increase or decrease in mixtures of 5CB with various carboxylic acids depending on whether the additive had a rigid or flexible structure [9]. When a nonmesogenic excipient is added to the LCs displaying both nematic and smectic phases, a T_{I-N} shift is observed, and a change in the nature of the transition between nematic and smectic phases from second to first order [10,11]. These few examples show that a small amount of a nonmesogenic additive can dramatically change the corresponding liquid-crystal properties.

Among pharmaceuticals, one of the most studied liquid-crystalline materials is itraconazole (ITZ), an antifungal drug with strongly anisotropic rod-shaped molecules, displaying both nematic and smectic phases. This thermotropic LC transforms to a nematic phase at $T_{N-I} = 363$ K upon cooling from the melt. On further cooling, it converts to a smectic phase at $T_{SmA-N} = 347$ K. This sequence of phase transitions can be modified after appropriate thermal treatment. So the nematic to smectic transition can be avoided at a cooling rate exceeding 20 K/s [12]. The ability to alter the temperature of the

*Corresponding author: marzena.rams-baron@us.edu.pl

phase transitions in the binary systems containing ITZ and low (water [13], other antifungal drugs [14], octa-acetyl maltose [15]) and high (polymers [15]) molecular weight excipients was also reported. Recently, an exciting possibility of tuning the phase behavior of ITZ in a binary system with a nonmesogenic additive, glycerol (GLY), was reported [16]. As the GLY content increases, the temperature range corresponding to the nematic phase decreases, up to a critical GLY concentration of 5% w/w, for which the nematic phase in the ITZ-GLY mixture disappears completely. As a result, on cooling, a direct first-order transition from isotropic to smectic-A phase was observed. These results motivate us to go one step further and discuss how the addition of GLY impacts the molecular dynamics of the ITR-GLY mixture.

Thus, our paper aims to investigate the molecular dynamics of the ITZ-GLY mixture with the 5% w/w addition of GLY to provide an insight into the novel phase behavior using broadband dielectric spectroscopy (BDS). The previous high-resolution adiabatic scanning calorimetry study of the ITZ-GLY mixture showed that the isotropic to smectic transition in a binary system has a stronger first-order character than transitions observed in neat ITZ, with much higher transition heat involved [16]. Therefore, it is interesting to recognize the molecular dynamics of the ITZ-GLY mixture with 5% w/w of GLY where the character of phase transitions is different. We will show that the direct smectic-A to isotropic phase transition manifests itself clearly in the dielectric response of the system studied, allowing the exact determination of the transition temperature from the dielectric parameters. To confirm the direct smectic-A to isotropic phase transition we used polarized microscopy. In addition, infrared spectroscopy measurements were carried out which shed more light on the nature of molecular interactions between mixture components. For comparative purposes, dielectric data for ITZ-GLY mixtures with lower GLY content (1 and 2% w/w) will be also presented.

II. MATERIAL AND METHODS

A. Materials

ITZ with purity >98% and molecular mass $M_w = 705.64$ g/mol was purchased from Tokyo Chemical Industry Co., Ltd. This pharmaceutical is described chemically as 2-butan-2-yl-4-[4-[4-[4-[(2*R*,4*S*)-2-(2,4-dichlorophenyl)-2-(1,2,4-triazol-1-ylmethyl)-1,3-dioxolan-4-yl]methoxy]phenyl]piperazin-1-yl]phenyl]-1,2,4-triazol-3-one. GLY, i.e., propane-1,2,3-triol, with purity $\geq 99.5\%$ and molecular mass $M_w = 92.09$ g/mol was purchased from Sigma-Aldrich. The chemical structures of both materials are presented as insets in Fig. 1(a).

B. Preparation of ITZ-GLY mixture

To prepare a binary mixture of ITZ and GLY with a 1, 2, and 5% addition (w/w) of GLY, we reproduced the methodology proposed by Amponsah-Efah *et al.* [16]. The ITR was dissolved in dichloromethane at $T = 323$ K with sonication. The GLY was dissolved in methanol, after which both solutions were mixed. The solvents were rapidly evaporated at $T = 323$ K under reduced pressure in a rotary evaporator

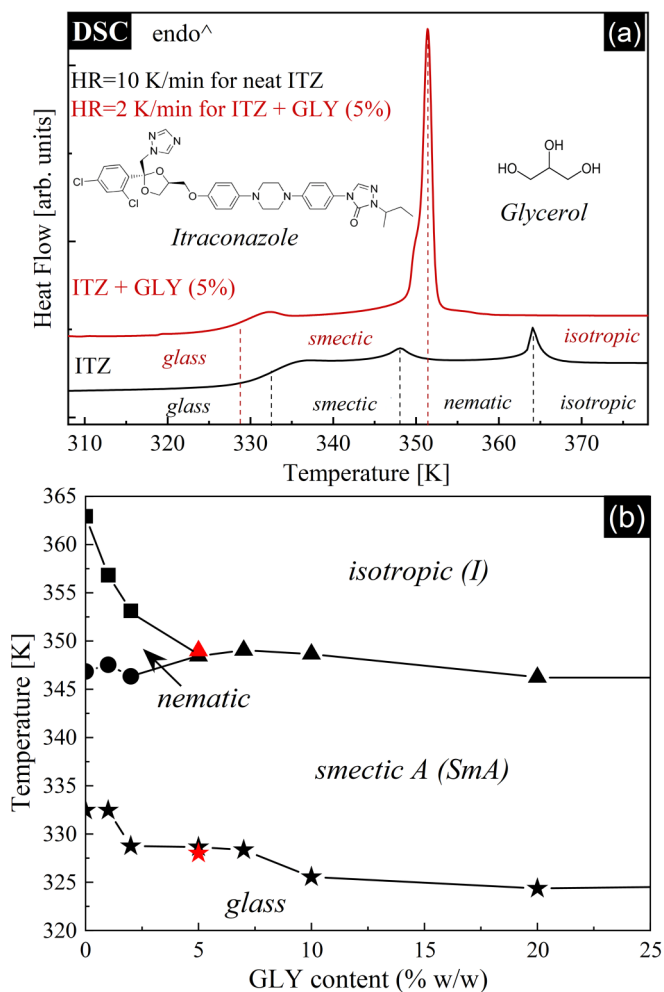


FIG. 1. (a) The comparison of DSC heating scans for neat ITZ and ITZ-GLY 5% w/w. (b) Phase diagram of ITZ-GLY mixture constructed from DSC data digitalized from [16] (depicted as black symbols). Our results for the ITZ-GLY sample with 5% w/w addition of GLY are shown as red symbols.

(Buchi Rotavapor R-100 with Vacuum Pump V-100 and Heating Bath B-100). Then the evaporation system was lightly ground using mortar and pestle.

C. Differential scanning calorimetry

The thermal properties of neat ITR, GLY, and ITR-GLY mixtures were investigated using the Mettler-Toledo differential scanning calorimetry (DSC) 1 STARe system. The measuring device was calibrated for temperature and enthalpy using zinc and indium standards. The measuring device was equipped with a ceramic HSS8 sensor with 120 thermocouples and a liquid nitrogen cooling station. The glass transition temperature (T_g) was determined as the midpoint of the glass transition step, while the liquid-crystal phase transition temperature was determined as the onset of the endothermic process. The samples were measured in an aluminum crucible (40 μ l). Pure substances were measured at a heating rate of 10 K/min in the temperature ranges from 283 to 453 K for ITR and 153 to 393 K for GLY. The ITR-GLY mixtures

were heated up with a rate of 2 or 10 K/min in the range of 153–453 K.

D. Polarized light microscopy

The optical texture observation was carried out using polarized optical microscopy (POM) and viewed through an Olympus BX50 polarizing microscope equipped with crossed polarizers. The microscope provided a heating stage (Linkam) and CCD camera to capture images and videos. The planar-aligned cells of thickness $9\ \mu\text{m}$ were used for texture observation. Samples of ITZ and ITZ-GLY mixture with 5% of GLY were filled into planar LC cells at the temperature 3 K above the clearing point with rubbed surfaces to induce director orientation parallel to the cell surface. POM images were recorded for observation of the texture evolution of the samples with temperature on cooling from isotropic phase down to glass transition.

E. Fourier transform infrared spectroscopy

Fourier-transform infrared (FTIR) spectroscopy measurements of ITZ and ITZ-GLY mixture with 5% of GLY were carried out using an Agilent Cary 640 FTIR spectrometer equipped with a GladiATR diamond accessory (Pike Technologies) in the $4000\text{--}400\text{-cm}^{-1}$ range. Each spectrum was an average of 32 scans recorded at a resolution of $2\ \text{cm}^{-1}$.

F. Broadband dielectric spectroscopy

Dielectric measurements in a wide temperature range (from 153 to 413 K) with step intervals of 10 K for the region 153–325 and 2 K for temperatures above 327 K were performed using a Novocontrol GMBH Alpha analyzer with frequencies ranging from $f = 10^{-1}$ to 2×10^6 Hz. During measurements, the temperature was precisely controlled by a Quatro temperature controller using a nitrogen gas cryostat. The temperature was stabilized with an accuracy of 0.1 K. The sample was placed between stainless steel electrodes of the capacitor (15-mm diameter) with a fixed distance between electrodes (0.1 mm) provided by fused silica spacer fibers. Before measurement the evaporated ITZ-GLY mixture was vitrified by melting at $T = 453\ \text{K}$ followed by a rapid supercooling on a copper plate.

III. RESULTS AND DISCUSSION

To prepare the ITZ-GLY binary mixtures with 5% w/w addition of GLY, we followed the solvent evaporation procedure described by Amponsah-Efah *et al.* [16]. The phase behavior of the sample was then tested using the DSC method. Thermograms recorded for a sample with 5% w/w addition of GLY vitrified *in situ* in the DSC apparatus are presented in Fig. 1(a) together with the data for neat ITZ. The reheating scans for the ITZ-GLY mixture with 5% of GLY revealed one additional endothermic process apart from the glass transition event. This fact is interesting considering that in the case of neat ITZ two LC phase transitions (i.e., T_{N-I} and $T_{\text{SmA}-N}$) appear. As shown in Fig. 1(a) heating (2 K/min) above the glass transition temperature, T_g , transforms the smectic-A phase of the ITZ-GLY sample directly to the isotropic liquid, omitting

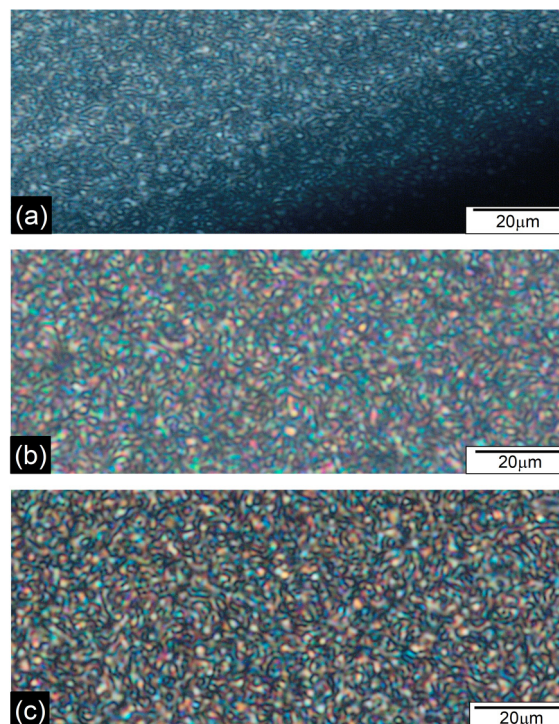


FIG. 2. (a) Isotropic-to-smectic-A transition observed under POM for ITZ-GLY mixture 5% w/w at $T = 350\ \text{K}$. (b) Smectic-A phase with a characteristic fan-shaped (focal-conic) texture viewed by POM for ITZ-GLY mixture 5% w/w at $T = 348\ \text{K}$ and neat ITZ (c) at $T = 340\ \text{K}$.

the nematic phase. The glass and smectic-A to isotropic transitions for mixture with 5% of GLY were observed at $T_g^{\text{DSC}} = 328\ \text{K}$ and $T_{\text{SmA}-I}^{\text{DSC}} = 349\ \text{K}$, respectively. These transition temperatures and the observed enthalpy changes are in perfect agreement with the previous data [16] [see Fig. 1(b)].

To confirm the presence of the smectic-A phase and an occurrence of a direct smectic-A to isotropic phase transition in the ITZ-GLY mixture with 5% of GLY we used polarized optical microscopy. POM images acquired for neat ITZ and mixture with 5% of GLY are shown in Fig. 2. The confocal texture of the smectic-A, which evolved into a mosaiclike texture, was observed near the clearing point where droplets began to form. This shows that chirality is transferred to the liquid crystal after the addition of GLY. The GLY molecules may be connected to the mesogenic core via hydrogen bonds resulting in the formation of a chiral smectic phase. The texture exhibited an intense blue-green color, but with the focal coniclike features of the smectic-A phase, remaining intact down to the glassy phase.

Although the substantial impact of GLY on the character of phase transition in the ITZ drug was reported before, the question of *how the presence of GLY affects the liquid-crystalline order of ITZ* remains unresolved. To shed more light on this issue we carried out FTIR measurements in a wide range of temperatures, i.e., from 293 to 358 K. FTIR spectra of ITZ, GLY, and ITZ-GLY mixture with 5% of GLY at $T = 293$ and $358\ \text{K}$ are shown in Fig. 3. A spectrum of GLY shows a broad band at $3271\ \text{cm}^{-1}$, which corresponds to the stretching vibration of hydrogen-bonded OH groups.

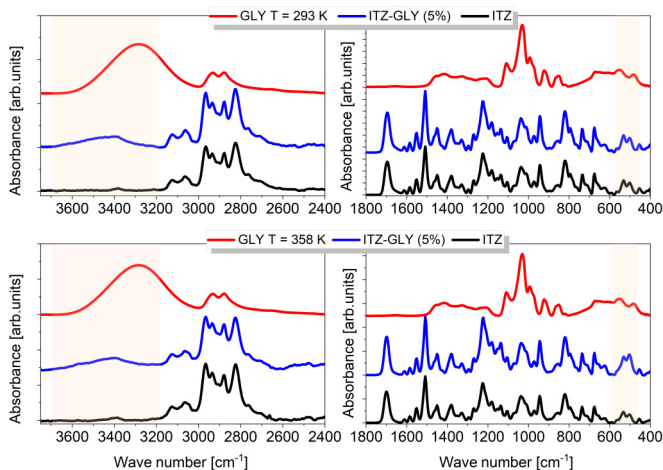


FIG. 3. Infrared spectra of GLY (red), ITZ (black), and ITZ-GLY mixture with 5% of GLY (blue) being measured at (upper) 293 K and (bottom) 358 K. Data are presented in two spectral regions: (left) 3750–2400 cm^{-1} and (right) 1800–400 cm^{-1} .

On the other hand, a very weak peak at 3382 cm^{-1} attributed to the C = O overtone is observed in the spectrum of ITZ, which means that no association process (by strong hydrogen bond interactions) occurs between ITZ molecules. The FTIR spectrum of the ITZ-GLY mixture 5% w/w closely resembles that of the ITZ sample. Both spectra differ only at two spectral regions, i.e., (1) 3700–3200 cm^{-1} and (2) 580–470 cm^{-1} . For the mixture, a broad band of low intensity appearing in region 1 is detected. What is more, the maximum of this band is shifted towards higher frequencies relative to that in GLY, which can be directly correlated with the formation of weak H-bonding interactions between both components. In turn, the spectral behavior of the peaks in region 2, originating from the C-Cl stretching vibrations [17], during heating differs for ITZ and its mixture with GLY (see Fig. 4). For ITZ, with an increasing temperature, a change in the intensity ratio of the doublet components is observed, especially in

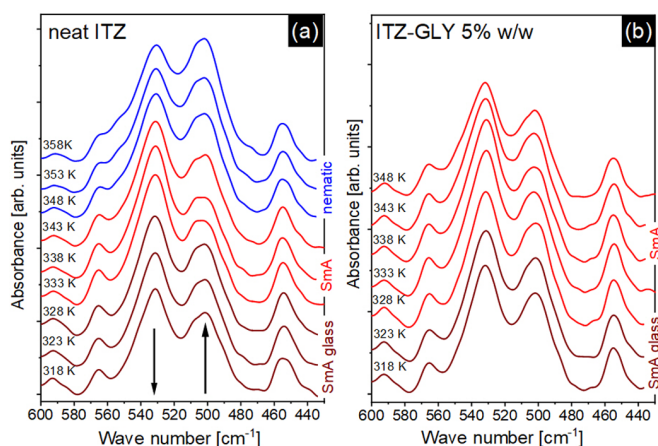


FIG. 4. Temperature-dependent FTIR spectra of (a) ITZ and (b) ITZ-GLY mixture with 5% of GLY in the frequency range of 600–430 cm^{-1} . The spectra were shown on a common scale, offset for clarity.

the temperature range of 338–358 K, i.e., the intensity of the peak at $\approx 530 \text{ cm}^{-1}$ decreases, whereas that at 500 cm^{-1} increases. This indicates the difference in intermolecular interactions (C–Cl...O contacts) between molecules in these temperatures. This fact corresponds well with the crystallographic data for the ITZ, which confirmed the existence of a weak halogen bond (C–Cl...O) between drug molecules [18]. On the other hand, there were no significant changes in the intensity ratio of the doublet components for the examined mixture as the temperature increases. This means that the addition of GLY inhibits the reorganization of ITZ molecules upon heating by changing the way the molecules interact *via* halogen bonds. In such conditions the nematic order cannot be stabilized at temperatures above the smectic-A phase and the system transforms directly to the isotropic phase.

To get insight into molecular dynamics of the ITZ-GLY mixture with 5% w/w addition of GLY, we measured the dielectric spectra for a melt-quenched sample in a broad temperature range covering glassy, smectic-A, and isotropic phases of a sample. The frequency behavior of the real, ϵ' , and imaginary, ϵ'' , parts of a complex dielectric permittivity $\epsilon^* = \epsilon' - i\epsilon''$ at different temperatures is shown in Fig. 5.

Since the effective intermolecular potential of LCs consists of distance-dependent and orientation-dependent parts, the dynamics displayed by LCs in the isotropic and liquid-crystalline phases can vary significantly [19,20]. When looking at the spectra in Figs. 5(a) and 5(b), two temperature regions at $T > T_g$ can be distinguished where the observed pattern of dielectric response is different. Above $T = 349 \text{ K}$, i.e., at the temperature corresponding to the calorimetric smectic-A to isotropic phase transition ($T_{\text{SmA-I}}^{\text{DSC}} = 349 \text{ K}$), an abrupt change in the magnitude of the main peak can be seen. Additionally, from $\epsilon''(f)$ data, a change in the temperature sensitivity of the primary relaxation below and above $T = 349 \text{ K}$ can be deduced. The inspection of $\epsilon'(f)$ data reveals a step change of parameters as well. In the low-frequency part of the $\epsilon'(f)$ spectrum some fluctuations of the static permittivity were detected [see Fig. 5(d)]. These might be due to the substantial variations in the molecular alignment during the ongoing LC transition and the appearance of various forms of local order leading to the fluctuations of a dipole moment. For neat ITZ such effects were not reported [21]. Also for ITZ mixtures with lower GLY content (1 and 2% w/w), such effects were not detected (see Supplemental Material [22]). But in these cases, the changes in the arrangement of the molecules accompanying the observed transition were less spectacular because they were mediated by the nematic phase. The change from the smectic-A to nematic alignment and the transition from the nematic to isotropic phase in neat ITZ and ITZ-GLY mixtures with 1 and 2% of GLY did not impact the dielectric response as much as it was observed for mixture with 5% of GLY, where the substantial changes in positional and orientational order occur simultaneously. To recognize these intriguing effects more deeply a fitting analysis was carried out. The dielectric loss spectra were analyzed in terms of the Havriliak-Negami equation [23]:

$$\epsilon^*(\omega) = \epsilon_\infty + \sum_{i=1}^n \frac{\Delta\epsilon}{[1 + (i\omega\tau_{\text{HN}})^\alpha]^\beta} + \frac{\sigma_{\text{DC}}}{\epsilon_0 i\omega},$$

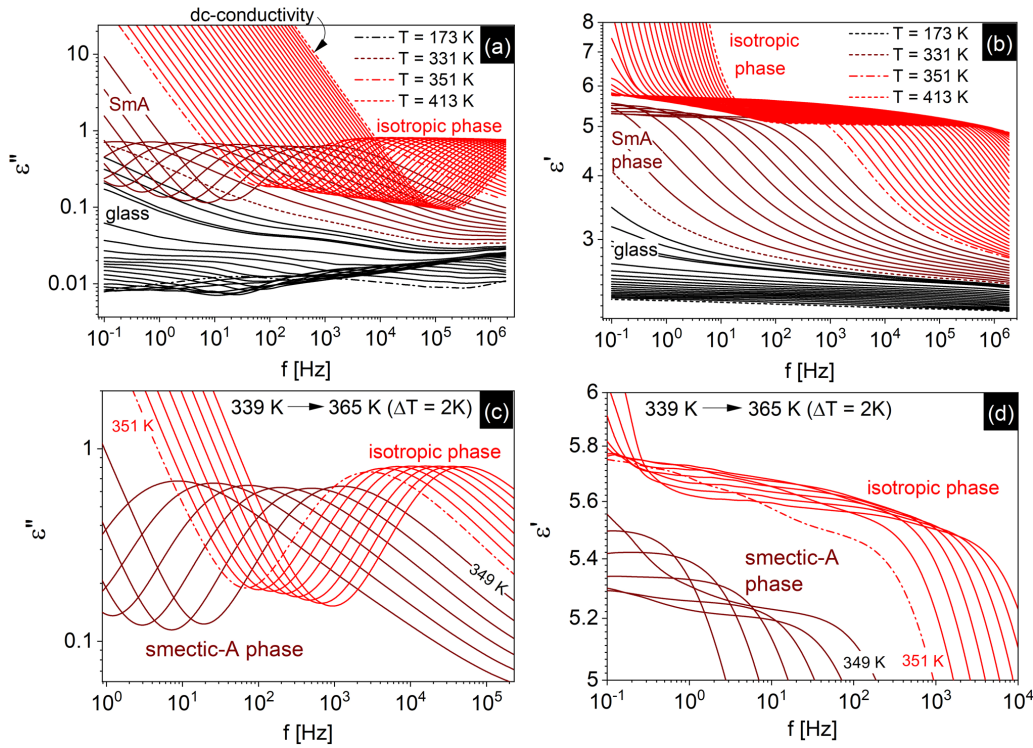


FIG. 5. Dielectric loss (a) and dispersion (b) spectra for the ITR-GLY mixture (5% GLY w/w) in the temperature ranges from 173 to 323 K (with $\Delta T = 10$ K) and from 325 to 413 K ($\Delta T = 2$ K). The bottom panel shows the variation of the real (d) and imaginary (c) parts of dielectric permittivity with a frequency in the selected temperatures near the smectic-A to isotropic phase transition.

where $\omega = 2\pi f$ is an angular frequency, ϵ_∞ is the dielectric constant in the high-frequency limit, ϵ_0 is a static permittivity of a vacuum, $\Delta\epsilon$ is the relaxation strength, and τ_{NH} is a characteristic HN-relaxation time. Exponents α and β are shape parameters. The term $\sigma_{DC}/\epsilon_0 i\omega$ takes into account the DC-conductivity (σ_{DC}) contribution that affects the dielectric response of ITZ-GLY at lower frequencies [see Fig. 5(a)]. The dielectric loss spectra for the ITZ-GLY mixture with 5% of GLY w/w at $T > T_g$ have been well described by combining two fitting functions with the DC-conductivity term. Attempts to analyze the loss data with a single function did not give satisfactory effects. Figure 6 shows the results of analysis for spectra registered at $T = 345$ K (smectic phase) and 353 K (isotropic phase) with marked areas of poor fit compliance. At $T < 351$ K, the excellent agreement was ensured by including an additional Debye-shaped ($\alpha = 1, \beta = 1$) relaxation process on the low-frequency shoulder of the prominent peak. Above 351 K, the primary process was well parametrized by a single function, but an excess contribution was visible in the DC-conductivity region. In this case, the slower Debye-shaped relaxation mode could be resolved after DC-conductivity subtraction (see inset in the right bottom panel of Fig. 6). In both cases, the low-frequency contribution will be described as α' , while the faster process will be assigned as α . Their molecular origin will be clarified in subsequent sections.

The relaxation dynamics of molecules with anisotropic geometry, such as ITZ, differ from that observed for isotropic systems the physical properties of which do not depend on the direction of measurement. From the point of view of dielectric measurements, an essential consequence of the elongation

of rod-shaped or disc-shaped particles is anisotropy of their electrical properties, which underlies the complex dielectric response [24]. The complex dielectric permittivity is then a tensorial quantity with two principal components being measured parallel, $\epsilon_{||}$, or perpendicular, ϵ_{\perp} , to the unique internal molecular axis called a director [25,26]. In the molecular

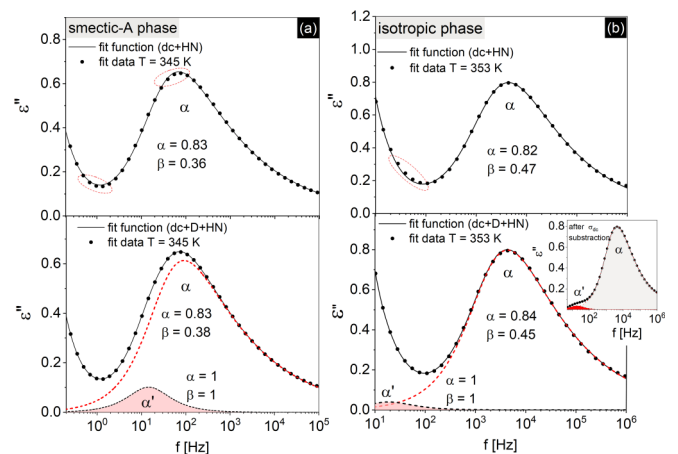


FIG. 6. Comparison of different fitting strategies to dielectric loss spectra for ITZ-GLY sample (5% GLY w/w) at $T = 345$ K (smectic phase) and $T = 353$ K (isotropic phase). The upper panels show the analysis results with a single HN function, and the bottom panels with a combination of the D and HN functions. In both cases, the fitting function included the DC-conductivity term. Symbols denote experimental data, solid lines denote resultant fit, and dashed lines denote individual components of the fit.

theories of LCs, the permittivity values are related to the correlation functions of the longitudinal and transverse components of the molecular dipole vector [25]. These theories were pioneered by Maier and Saupe [27–30], who gave expressions for the dielectric permittivity parallel and perpendicular to the director for an aligned uniaxial LC taking into account the molecular dipole moment and the orientational order parameter, S . This theory was further developed by Nordio *et al.* [31] and continued by others [32,33]. Readers interested in the theoretical background of dielectric relaxation of LCs are referred to [25,26,34] where more details are given. The main conclusion of these theoretical approaches is that the measured dielectric function parallel and perpendicular to the director includes different weighted sums of the four relaxation processes being characterized by different relaxation times and intensities governed by the macroscopic orientation of the sample. Depending on the character of molecular motions, the different contributions of dipole moment components variously affect the permittivity values, giving rise to the different dynamical responses to an external electric field [24].

The molecular dynamics of pure ITZ have been well recognized in recent years [6,21,35,36]. Two relaxation processes were observed on the dielectric loss spectra of ITZ in the liquid-crystalline phases and isotropic phases. The low-frequency mode, with minor amplitude, usually assigned as the δ mode, is attributed to the rotation about the short molecular axis (also described as flip-flop motions). The second process, dominating the dielectric response of ITZ in all phases, is ascribed to the faster rotation about the long axis. The relaxation times and glass transition temperature determined from the analysis of BDS data for the faster process are in good agreement with the corresponding calorimetric parameters established using the stochastic temperature-modulated DSC method [21]. Therefore, it is described as α relaxation, analogous to the structural relaxation in conventional glass-forming liquids. A significant disproportion in the intensity of both modes (the amplitude of the δ mode is only a small fraction of the amplitude of α -process) becomes clear when the components of the dipole moment vector are taken into consideration. According to DFT calculations reported by Tarnacka *et al.* the component of the dipole moment, μ , directed parallel to the long molecular axis of a molecule is much higher than the other components (μ along the semimajor axis x is 1.15 D, while the components parallel to the semiaxial y and z axes are $\mu = 0.42$ and 0.41 D) [21]. Consequently, the rotation about the long axis of the ITZ molecule contributes more to the dielectric response. The fact that the δ relaxation, intrinsically related to the anisotropic nature of ITZ, persists in the isotropic phase deserves a brief comment. In most materials displaying liquid-crystalline phases when the system enters the disordered isotropic liquid state the slow and fast modes fuse into a single broad relaxation process [37,26]. The unusual behavior of ITZ, observed in bulk [21] and confined samples [36], is thus regarded as experimental evidence for the existence of ordered domains that have outlasted despite the transition to the isotropic phase.

The temperature dependence of the relaxation times for slow and fast processes in the ITZ-GLY mixture is shown in Fig. 7. The values of relaxation times (τ_α , $\tau_{\alpha'}$, τ_β , τ_γ) were determined from the fitting parameters of the HN equation

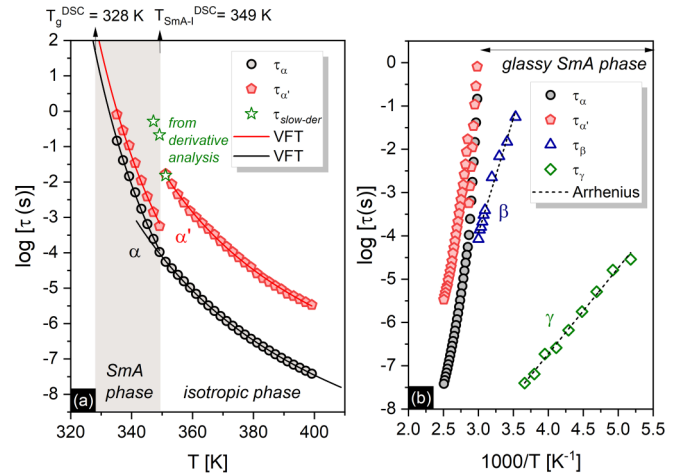


FIG. 7. Temperature dependence of the relaxation times determined for relaxation processes in glassy, smectic-A (SmA), and isotropic phases of ITZ-GL mixture with 5% of GLY. The solid and dashed lines show the fit of the VFT and Arrhenius fit functions, respectively. The temperature regions corresponding to the particular phases are distinguished according to DSC measurements.

using the following relationship [26]:

$$\tau = \tau_{\text{HN}} \left[\sin\left(\frac{\pi\alpha}{2+2\beta}\right) \right]^{-1/\alpha} \left[\sin\left(\frac{\pi\alpha\beta}{2+2\beta}\right) \right]^{1/\alpha}.$$

The changes in the character of the temperature dependence of τ_α and $\tau_{\alpha'}$ in the smectic-A and isotropic phase transition can be seen. The faster rotations were less affected by changes in molecular alignment than the α' process. In the case of α relaxation, a change in the steepness of $\tau_\alpha(T)$ can be noted in the smectic-A and isotropic phases. In contrast, for the α' process, an apparent discontinuity in the $\tau_{\alpha'}(T)$ dependency was observed. Interestingly, the molecular motions related to the slow α' mode appear to be accelerated in the ordered smectic-A phase, as indicated by their sudden slowing down as the system enters the disordered isotropic phase.

To interpret the origin of the relaxation processes in the ITZ-GLY mixture with 5% of GLY we compared our data with those for the neat ITZ. Figure 8 compares the loss spectra for the ITZ-GLY mixture and ITZ under isochronic (i.e., different temperatures but constant relaxation time τ_α) conditions. The spectral shape was found to be almost identical. Thus, the same molecular origin of relaxation processes is highly possible. Accordingly, the α' and α modes on the dielectric loss spectra of the ITZ-GLY mixture with 5% of GLY could be ascribed to the ITZ molecule's rotational motion about the short and long axes, respectively.

Simultaneously, when such an assignment is done, from the data depicted in Fig. 7(a), one can deduce that the molecular arrangement in ordered smectic-A layers would facilitate the α' process and speed up the rotations around the short axes of the ITZ molecule. The abrupt slowing down of dynamics associated with α' , indicated by the steplike increasing of the $\tau_{\alpha'}$ when entering the isotropic phase, is surprising. It is intuitively expected that the motions of molecules organized in smectic-A layers and impeded by high potential barriers

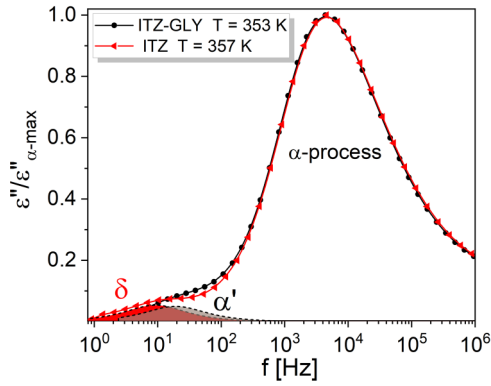


FIG. 8. The comparison of dielectric loss spectra for ITZ and ITZ-GLY mixture with 5% of GLY at the isochronic condition (for the same τ_α). The spectra were normalized to the maximum of the α peak. The DC conductivity has been subtracted.

will be slower than in the isotropic phase, not faster, as we observed here. In addition to the above, the comparison of dielectric loss spectra for ITZ and the ITZ-GLY mixture with 5% of GLY at temperatures corresponding to the smectic-A phase also shows substantial differences (see Fig. 9). A possible explanation for this peculiar behavior is that the α' mode observed in the smectic-A phase should not be considered as a continuation of the low-frequency mode observed in the isotropic phase. Due to the greater DC conductivity in the ITZ-GLY sample [compared to neat ITZ, see Fig. 9(a)], the observation of additional low-frequency relaxation (being equivalent of the δ mode in ITZ) in the temperature regime corresponding to the smectic-A phase might be hindered. Then

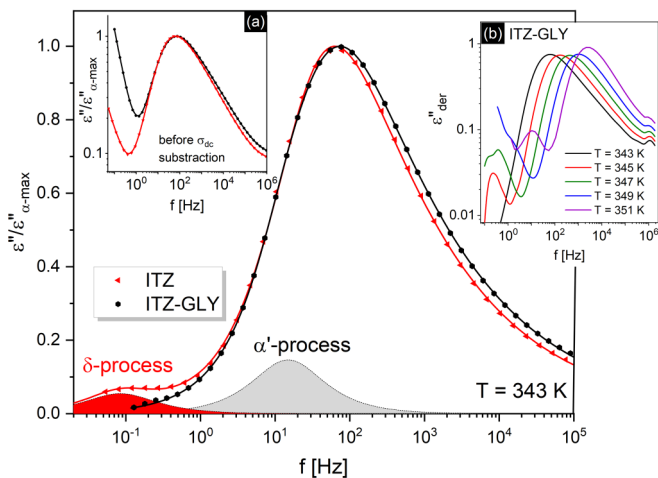


FIG. 9. The comparison of dielectric loss spectra measured for ITZ and ITZ-GLY mixture at $T = 343$ K corresponding to the smectic-A phase. The spectra were normalized to the maximum of the α peak. The DC conductivity has been subtracted. The position of low-frequency modes for ITZ and ITZ-GLY is indicated as δ and α' , respectively. The inset shows (a) the comparison of dielectric loss spectra before DC-conductivity subtraction and (b) calculated loss spectra for temperatures close to smectic-A to isotropic transition; instead measuring $\epsilon''(f)$ the $\epsilon''_{\text{der}}(f)$ data are presented where conductivity contribution is eliminated.

fitting the $\epsilon''(f)$ data is not conclusive. Thus, we analyzed the data calculated from $\epsilon'(f)$ spectra using the derivative method yielding $\epsilon''_{\text{der}}(f) \approx -(\pi/2) \times [\partial\epsilon'(f)/\partial\ln f]$ [38]. These results, presented in Fig. 9(b), show that at temperatures $T > 343$ K the process slower than α' can be hidden under the DC conductivity. Due to the low resolution, its parametrization was difficult. Still, we estimated the relaxation times [from the maximum of the low-frequency peak in $\epsilon''_{\text{der}}(f)$ data], depicted as green stars in Fig. 7(a). The inspection of data presented in Fig. 7(a) reveals that the relaxation times estimated from the derivative data ($\tau_{\text{slow-der}}$) seem to be a continuation of the $\tau_{\alpha'}(T)$ dependence determined from spectra registered in the isotropic phase. This means that the mechanism of the α' process observed in the smectic-A phase cannot be related to the short axes rotations, which appear to be much slower. The data presented in Fig. 7 portrayed a very similar course of $\tau_\alpha(T)$ and $\tau_{\alpha'}(T)$ in the smectic-A phase. This suggests that the actual energy barrier hindering both processes in the LC phase is almost similar. Thus, their molecular mechanism most probably will be the same. Moreover, in the isotropic phase, these modes overlap into a single relaxation process. In liquid-crystalline materials, the faster rotations around the long axis can be sensitive to various molecular aspects of the structure, such as a difference in flexibility [24]. Thus, the two processes observed on $\epsilon''(f)$ spectra for the ITZ-GLY mixture in the smectic-A phase and assigned as α' and α in Fig. 7 may reflect rotations of different molecular fragments around the long axis variously affected by the smectic-A order.

The data presented in Fig. 7 show that the liquid-crystalline order substantially influences the character of temperature dependencies of relaxation times in the ITZ-GLY mixture with 5% of GLY. In the smectic-A phase, the temperature dependence of the relaxation times associated with both α and α' processes has a much steeper course compared to the isotropic phase and almost linear character. Nevertheless, a good parametrization with the Vogel-Fulcher-Tammann (VFT) function [39–41] was possible. The fit parameters τ_0 , D , and T_0 obtained by fitting the data in Fig. 4(a) to the equation $\tau_\alpha(T) = \tau_\infty \exp[DT_0/(T-T_0)]$ are summarized in Table I. The similar fitting parameters for α and α' processes in the smectic-A phase suggest that both types of motions might be coupled. It is also evidenced by the similar temperature in which both processes become frozen when approaching a glassy phase. According to the condition that defines the glass transition, i.e., $\tau(T = T_g) = 100$ s, this will happen at $T = 327.3$ K for the α process and $T = 329.2$ K for the α' process. In ITZ the fast α process attributed to the rotational fluctuations of the molecule around its long axis was associated with the glass transition detected by DSC measurements [12,21]. We expected the same for mixtures. However, the slight differences between the temperatures at which the α and α' dynamics are frozen do not allow us to state this unequivocally.

When the material fluidity is lost below T_g and the timescale of cooperative rearrangements is much longer than the experimental time scale, the relaxation response of the ITZ-GLY sample is dominated by secondary modes. As in the case of neat ITZ, two secondary relaxations were visible on the loss spectra of the ITZ-GLY mixture, marked as β and

TABLE I. The summary of VFT and Arrhenius fitting parameters for ITZ-GLY mixture with 5% of GLY.

Process	Smectic-A phase			Isotropic phase ($T > 351$ K)			Glassy smectic-A phase	
	$\log \tau_\infty$	D	T_0 (K)	$\log \tau_\infty$	D	T_0 (K)	$\log \tau_\infty$	E_a (kJ/mol)
α	-14.0^a	4.7	290.2	-13.0	6.3	267.2		
α'	-14.0^a	5.3	287.5	-10.5	4.6	285.8		
β							-19.8	101.5 ± 4.9
γ							-14.7	38.0 ± 1.1

^aFixed parameter.

γ processes. Their relaxation times follow an Arrhenius-type temperature dependence, shown in Fig. 7(b). The activation energy barrier values, E_a , were obtained by fitting the equation $\tau = \tau_\infty \exp(E_a/RT)$ to the experimental data in Fig. 7(b), where τ_∞ is the preexponential factor, and R is the gas constant, given in Table I. The values of $E_a = 101.5 \pm 4.9$ and 38.1 ± 1.1 kJ/mol for β and γ modes, respectively, are similar to those reported for pure ITZ, i.e., 93.8 ± 1.5 (β process) and 36.2 ± 1.9 (γ process) [15]. This means that the 5% w/w addition of GLY, although it significantly impacts the character of liquid-crystalline phase transitions in the ITZ-GLY mixture, does not change remarkably the system's behavior in the glassy state.

From the data presented so far, it is clear that the analysis of dielectric data for the ITZ-GLY mixture with 5% of GLY allows determining the temperature of the smectic-A to isotropic transition with high accuracy. The variation in the degree of molecular order leaves a clear fingerprint on the temperature behavior of the relaxation times for both the faster and the slower processes. The intersection of the VFT fit functions for the α process in the smectic-A and isotropic phases and the step change in the relaxation times related to the rotational motions around a short axis (described by $\tau_{\alpha'}$ in the isotropic phase and $\tau_{\text{der-slow}}$ in the smectic-A phase) correspond perfectly to the phase transition temperature determined in calorimetric studies $T_{\text{SmA-I}}^{\text{DSC}} = 349$ K. On the other hand, for pure ITZ and mixtures with a lower GLY content (1 and 2% w/w), such changes were less pronounced (see Fig. 10). As shown in Fig. 10(a) for ITZ-GLY mixture with 1% of GLY to find the evidence of LC transitions observed in DSC measurements the data linearization via the derivative of the experimental $\log \tau_\alpha$ values with respect to temperature was necessary.

For the mixture with 5% of GLY, the temperature at which the smectic order disappears and the system enters the isotropic state can be determined from the analysis of the temperature dependency of other dielectric parameters. Figure 11 shows the changes in DC conductivity (σ_{DC}), dielectric strength ($\Delta\epsilon$) of α relaxation, and shape parameters of the HN function for α relaxation (the slower process was assumed to be Debye shaped) during reheating of ITZ-GLY mixtures with different GLY content. For a sample with 5% of GLY, the values of σ_{DC} and $\Delta\epsilon$ turned out to be very sensitive to changes in the molecular organization. Consequently, the analysis of temperature evolution of σ_{DC} and $\Delta\epsilon$ allows determining the temperature of smectic-A to isotropic phase transition with good accuracy. For samples with lower GLY content, only $\Delta\epsilon$ was found to be sensitive to LC transitions. The evident changes in the character of $\Delta\epsilon(T)$ occurred near

the calorimetric $T_{\text{SmA-N}}^{\text{DSC}}$ and $T_{\text{N-I}}^{\text{DSC}}$. In DSC measurements (with heating rate 10 K/min) for a sample with 1% of GLY the smectic-A to nematic transition was observed at $T_{\text{SmA-N}}^{\text{DSC}} = 348$ K while the nematic to isotropic phase transition was observed at $T_{\text{N-I}}^{\text{DSC}} = 356$ K. For a mixture with 2% of GLY, these LC transitions were observed at $T_{\text{SmA-N}}^{\text{DSC}} = 349$ K and $T_{\text{N-I}}^{\text{DSC}} = 354$ K, respectively.

The data in Fig. 11(b) for a mixture with 5% of GLY show a sudden increase in the dielectric strength upon transition to the isotropic phase. The observed growth of $\Delta\epsilon$ manifests an increase of effective dipole moment due to dipole randomization. This means that in the smectic-A phase, the dipole moments of individual layers are oppositely directed, forming a structure with a partially canceled dipole moment. When this ordered molecular array collapses while entering the disordered liquid state, antiparallel correlations between molecules are weakened, and the resultant dipole moment of a system increases. Apart from the discontinuity in the $\Delta\epsilon(T)$, the atypical temperature behavior of $\Delta\epsilon$ is portrayed by data in Fig. 11(b). Above 351 K instead of a decrease of $\Delta\epsilon \sim \mu^2/kT$ on heating, its gradual increase was recorded in the range of 8 K above the transition temperature. Such a

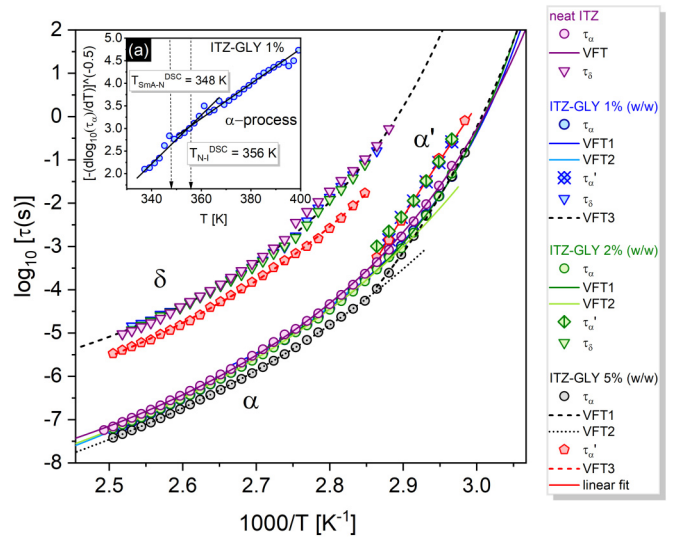


FIG. 10. Relaxation map for ITZ and ITZ-GLY mixtures with different GLY content at temperatures corresponding to smectic-A, nematic, and isotropic phases. (a) Results of the linearized derivative-based analysis of the temperature dependence of structural relaxation time for mixture with 1% of GLY. Arrows denote temperatures at which endothermic LC transitions were observed in DSC measurements.

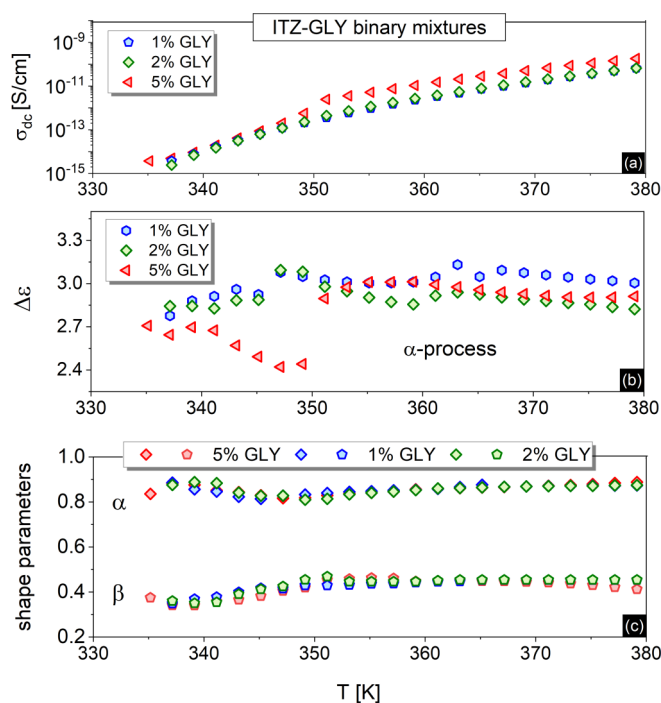


FIG. 11. The temperature evolution of (a) DC conductivity, σ_{DC} , (b) dielectric strength, $\Delta\epsilon$, characterizing α relaxation, and (c) shape parameters of the HN function for α relaxation observed for ITZ-GLY mixtures with different GLY content.

transition-related anomaly in the temperature dependence of static permittivity, observed for some LCs [42–46], can be rationalized by the presence of ordered domains in the isotropic phase that strongly impact the system dynamics [47,48]. The Landau–de Gennes theory describing the dynamics of a system approaching nematic to isotropic phase transition from above assumes that the local nematiclike order responsible for these unusual effects exists in the material on a distance scale defined by correlation length ζ [47,49]. Consequently, such unique dynamical effects may be observed even ≈ 50 K above a transition temperature [50].

IV. CONCLUSIONS

The paper aimed to investigate the molecular dynamics of the ITZ-GLY mixture with a 5% w/w addition of GLY using BDS spectroscopy. According to the previous report [16], such a concentration of GLY significantly modified the ITZ drug’s liquid-crystalline properties. In the investigated mixture, the nematic phase was eliminated, and on heating, after leaving the smectic-*A* phase, the system directly enters the disordered isotropic state. Our dielectric study of the melt-quenched ITZ-GLY mixture revealed several relaxation processes in the glassy, smectic-*A*, and isotropic phases and

showed exciting facts about the impact of GLY on the system dynamics. It turned out that the addition of GLY affects to a lesser extent the dynamics of the system in the isotropic and glassy phases leading to a similar relaxation response as in the case of neat ITZ. The spectacular effects associated with the addition of GLY were revealed in (i) the sequence of the phase transitions (excluding the nematic phase), (ii) the pattern of relaxation processes in the smectic-*A* phase, and (iii) the relaxation behavior at the liquid-crystalline and isotropic liquid state boundary. In the investigated system, we studied the direct transition from the ordered smectic-*A* phase to the randomly organized isotropic phase, which had a clear and measurable effect on the dielectric response. This phenomenon deserves to be studied further, mostly as it cannot be observed in neat ITZ, where the transition between LC and conventional liquid states is more gradual as it passes through the nematic phase. It is essential from the pharmaceutical point of view because the ability to control the degree of liquid-crystalline order is directly related to the amorphous drugs’ stability and solubility issues. It is also exciting from the perspective of fundamental studies of critical phenomena in soft matter. Our analysis of the $\epsilon''(f)$ spectra revealed the presence of two relaxation processes in the smectic-*A* phase with similar temperature dependencies of relaxation times, suggesting a similar molecular mechanism (most probably rotational motions around the long axis). Although initially suspected, the slower process does not seem to correspond to the δ process observed for neat ITZ. A more detailed derivative analysis indicated that the DC-conductivity contribution could obscure this slow mode counterpart in the smectic-*A* phase. At higher temperatures corresponding to the liquid state, its presence on the dielectric loss spectra of the ITZ-GLY mixture is detectable and indisputable. We show that the smectic-*A* to isotropic phase transition in the investigated mixture is manifested in the dielectric loss and dispersion spectra. The differences in the molecular dynamics below and above the transition temperature are so pronounced that the transition temperature can be easily recognized from dielectric data with good accuracy with DSC results. We show that the disappearance of the liquid-crystalline order leaves a clear fingerprint on the temperature behavior of various spectral parameters (relaxation times, $\Delta\epsilon$, and σ_{DC}). It presents vast potential for further studies on phase transitions in the ITZ-GLY system at conditions where the application of the DSC technique is limited, e.g., under high pressure.

ACKNOWLEDGMENT

M.R.-B., J.K.-K., and M.P. are grateful for the financial support received within Project No. 2015/16/W/NZ7/00404 (SYMFONIA 3) from the National Science Centre.

- [1] P. K. Mukherjee, Isotropic to smectic-*A* phase transition: A review, *J. Mol. Liq.* **190**, 99 (2014).
 [2] D. Andrienko, Introduction to liquid crystals, *J. Mol. Liq.* **267**, 520 (2018).

- [3] J. P. F. Lagerwall and G. Scalia, A new era for liquid crystal research: Applications of liquid crystals in soft matter nano-, bio- and microtechnology, *Curr. Appl. Phys.* **12**, 1387 (2012).

- [4] C. Grigoriadis, H. Duran, M. Steinhart, M. Kappl, H. J. Butt, and G. Floudas, Suppression of phase transitions in a confined rodlike liquid crystal, *ACS Nano* **5**, 9208 (2011).
- [5] J. B. Marlow, T. M. McCoy, C. Q. Ho, L. De Campo, R. Knott, T. D. M. Bell, and R. F. Tabor, Tuning the structure, thermal stability and rheological properties of liquid crystal phases: Via the addition of silica nanoparticles, *Phys. Chem. Chem. Phys.* **21**, 25649 (2019).
- [6] J. Knapik-Kowalczyk, K. Jurkiewicz, A. Kocot, and M. Paluch, Rheo-dielectric studies of the kinetics of shear-induced nematic alignment changes in itraconazole, *J. Mol. Liq.* **302**, 1 (2020).
- [7] H. K. Bisoyi and Q. Li, Light-driven liquid crystalline materials: from photo-induced phase transitions and property modulations to applications, *Chem. Rev.* **116**, 15089 (2016).
- [8] L. A. Serrano, M. J. Fornerod, Y. Yang, S. Gaisford, F. Stellacci, and S. Guldin, Phase behaviour and applications of a binary liquid mixture of methanol and a thermotropic liquid crystal, *Soft Matter* **14**, 4615 (2018).
- [9] V. Jirón and E. Castellón, Increased nematic-isotropic transition temperature on doping a liquid crystal with molecularly rigid carboxylic acids, *J. Phys. Chem. B* **124**, 890 (2020).
- [10] P. K. Mukherjee, Effect of nonmesogenic solute on the nematic-smectic-A phase transition, *J. Chem. Phys.* **116**, 9531 (2002).
- [11] P. K. Mukherjee and B. C. Khan, Nematic to smectic-A phase transition in mixture of liquid crystal and nonmesogenic impurities: Existence of tricritical point, *Liq. Cryst.* **46**, 1060 (2019).
- [12] R. Teerakapibal, C. Huang, A. Gujral, M. D. Ediger, and L. Yu, Organic Glasses with Tunable Liquid-Crystalline Order, *Phys. Rev. Lett.* **120**, 055502 (2018).
- [13] N. A. Mugheirbi, K. Fleischer, and L. Tajber, A rare case of mesomorphic behavior-molecular reorientation of itraconazole liquid crystal induced by a hygrothermal treatment, *Cryst. Growth Des.* **16**, 1329 (2016).
- [14] D. Heczko, E. Kamińska, K. Jurkiewicz, M. Tarnacka, K. Merkel, K. Kamiński, and M. Paluch, The impact of various azole antifungals on the liquid crystalline ordering in itraconazole, *J. Mol. Liq.* **307**, 112959 (2020).
- [15] E. Kaminska, M. Tarnacka, K. Kolodziejczyk, M. Dulski, D. Zakowiecki, L. Hawelek, K. Adrjanowicz, M. Zych, G. Garbacz, and K. Kaminski, Impact of low molecular weight excipient octaacetylmaltose on the liquid crystalline ordering and molecular dynamics in the supercooled liquid and glassy state of itraconazole, *Eur. J. Pharm. Biopharm.* **88**, 1094 (2014).
- [16] K. K. Amponsah-Efah, C. Glorieux, J. Thoen, and R. Suryanarayanan, Effect of glycerol on the order of the mesophase transitions of supercooled itraconazole, *J. Mol. Liq.* **320**, 114222 (2020).
- [17] G. Socrates, *Infrared Characteristic Group Frequencies: Tables and Charts*, 3rd ed. (Wiley, New York, 2001).
- [18] M. Lahtinen Nonappa, E. Kolehmainen, J. Haarala, and A. Shevchenko, Evidence of weak halogen bonding: new insights on itraconazole and its succinic acid cocrystal, *Cryst. Growth Des.* **13**, 346 (2013).
- [19] S. Urban and C. M. Roland, Low frequency relaxation in liquid crystals in relation to structural relaxation in glass-formers, *J. Non. Cryst. Solids* **357**, 740 (2011).
- [20] K. Koperwas, A. Grzybowski, and M. Paluch, Exploring the connection between the density-scaling exponent and the intermolecular potential for liquids on the basis of computer simulations of quasireal model systems, *Phys. Rev. E* **101**, 012613 (2020).
- [21] M. Tarnacka, K. Adrjanowicz, E. Kaminska, K. Kaminski, K. Grzybowska, K. Kolodziejczyk, P. Włodarczyk, L. Hawelek, G. Garbacz, A. Kocot, and M. Paluch, Molecular dynamics of itraconazole at ambient and high pressure, *Phys. Chem. Chem. Phys.* **15**, 20742 (2013).
- [22] See Supplemental Material at <http://link.aps.org/supplemental/10.1103/PhysRevE.104.034702> for dielectric loss and dispersion spectra of ITZ-GLY mixtures with 1 and 2% addition of GLY.
- [23] S. Havriliak and S. Negami, A complex plane representation of dielectric and mechanical relaxation processes in some polymers, *Polymer (Guildf)* **8**, 161 (1967).
- [24] D. Dunmur and G. Luckhurst, Liquid crystals, in *Springer Handbook of Electronic and Photonic Materials* (Springer, New York, 2006), pp. 917–951.
- [25] G. Williams, Dielectric relaxation behaviour of liquid crystals, in *The Molecular Dynamics of Liquid Crystals*, NATO ASI Series (Series C: Mathematical and Physical Sciences), Vol. 53 (Springer, New York, 1994), pp. 431–450.
- [26] F. Kremer and A. Schonhals, *Broadband Dielectric Spectroscopy* (Springer-Verlag, Berlin, 2003).
- [27] W. Maier and A. Saupe, Eine einfache molekulare theorie des nematischen kristallinflüssigen zustandes, *Z. Naturforsch, Teil A* **13**, 564 (1958).
- [28] W. Maier and G. Meier, Eine einfache theorie der dielektrischen eigenschaften homogen orientierter kristallinflüssiger phasen des nematischen typs, *Z. Naturforsch, Teil A* **16**, 262 (1961).
- [29] G. Meier and A. Saupe, Dielectric relaxation in nematic liquid crystals, *Mol. Cryst.* **1**, 515 (1966).
- [30] A. J. Martin, G. Meier, and A. Saupe, Extended debye theory for dielectric relaxations in nematic liquid crystals, *Symp. Faraday Soc.* **5**, 119 (1971).
- [31] P. Luigi Nordio, G. Rigatti, and U. Segre, Dielectric relaxation theory in nematic liquids, *Mol. Phys.* **25**, 129 (1973).
- [32] G. S. Attard, K. Araki, and G. Williams, A simple approach to the dielectric relaxation behaviour of a liquid crystalline polymer and its application to the determination of the director order parameter for partially aligned materials, *Br. Polym. J.* **19**, 119 (1987).
- [33] K. Araki, G. S. Attard, A. Kozak, G. Williams, G. W. Gray, D. Lacey, and G. Nestor, Molecular dynamics of a siloxane liquid-crystalline polymer as studied by dielectric relaxation spectroscopy, *J. Chem. Soc. Faraday Trans. 2* **84**, 1067 (1988).
- [34] D. A. Dunmur, M. R. de la Fuente, M. A. Perez Jubindo, and S. Diez, Dielectric studies of liquid crystals: The influence of molecular shape, *Liq. Cryst.* **37**, 723 (2010).
- [35] D. Heczko, E. Kamińska, M. Tarnacka, K. Jurkiewicz, M. Dulski, A. Bębenek, G. Garbacz, K. Kamiński, and M. Paluch, Varying thermodynamic conditions as a new way to tune the molecular order in glassy itraconazole, *J. Mol. Liq.* **286**, 1 (2019).
- [36] E. U. Mapesa, M. Tarnacka, E. Kamińska, K. Adrjanowicz, M. Dulski, W. Kossack, M. Tress, W. K. Kipnusu, K. Kamiński, and F. Kremer, Molecular dynamics of itraconazole confined in thin supported layers, *RSC Adv.* **4**, 28432 (2014).
- [37] M. Mierzwa, M. Rams-Baron, S. Capaccioli, S. Pawlus, and M. Paluch, How to align a nematic glassy phase–

- Different conditions–Different results, *J. Mol. Liq.* **280**, 314 (2019).
- [38] M. Wübbenhorst, E. M. Van Koten, J. C. Jansen, W. Mijs, and J. Van Turnhout, Dielectric relaxation spectroscopy of amorphous and liquid-crystalline side-chain polycarbonates, *Macromol. Rapid Commun.* **18**, 139 (1997).
- [39] H. Vogel, Das temperaturabhängigkeitgesetz der viskosität von flüssigkeiten, *J. Phys. Z.* **22**, 645 (1921).
- [40] G. S. Fulcher, Analysis of recent measurements of the viscosity of glasses, *J. Am. Ceram. Soc.* **8**, 339 (1925).
- [41] G. Tammann and W. Hesse, Die abhängigkeit der viskosität von der temperatur bie unterkühlten flüssigkeiten, *Z. Anorg. Allg. Chem.* **156**, 245 (1926).
- [42] A. Drozd-Rzoska, S. J. Rzoska, and J. Ziolo, Quasicritical behavior of dielectric permittivity in the isotropic phase of smectogenic n-cyanobiphenyls, *Phys. Rev. E* **61**, 5349 (2000).
- [43] J. Ziolo, J. Chrapeć, and S. J. Rzoska, Critical behavior of the isotropic–smectic-A transition in p-decyloxy-benzylidene-p-amino-2-methyl-butyl-cinnamate studied by the nonlinear dielectric effect method, *Phys. Rev. A* **40**, 448 (1989).
- [44] A. Drozd-Rzoska, S. J. Rzoska, and J. Ziolo, Critical behavior of dielectric permittivity in the isotropic phase of nematogens, *Phys. Rev. E* **54**, 6452 (1996).
- [45] M. J. Bradshaw and E. P. Raynes, Pre-transitional effects in the electric permittivity of cyano nematics, *Mol. Cryst. Liq. Cryst.* **72**, 37 (1981).
- [46] J. Jadżyn and G. Czechowski, Static dielectric pretransitional effects in thermotropic liquid crystals, *Opto-Electronics Rev.* **16**, 395 (2008).
- [47] H. Cang, J. Li, V. N. Novikov, and M. D. Fayer, Dynamics in supercooled liquids and in the isotropic phase of liquid crystals: A comparison, *J. Chem. Phys.* **118**, 9303 (2003).
- [48] J. J. Stankus, R. Torre, C. D. Marshall, S. R. Greenfield, A. Sengupta, A. Tokmakoff, and M. D. Fayer, Nanosecond time scale dynamics of pseudo-nematic domains in the isotropic phase of liquid crystals, *Chem. Phys. Lett.* **194**, 213 (1992).
- [49] P. G. De Gennes, Phenomenology of short-range-order effects in the isotropic phase of nematic materials, *Phys. Lett. A* **30**, 454 (1969).
- [50] S. D. Gottke, D. D. Brace, H. Cang, B. Bagchi, and M. D. Fayer, Liquid crystal dynamics in the isotropic phase, *J. Chem. Phys.* **116**, 360 (2002).